Bioresource Technology 103 (2012) 470–476

Contents lists available at SciVerse ScienceDirect

Bioresource Technology

journal homepage: www.elsevier.com/locate/biortech

Pyrolytic characteristics of biomass acid hydrolysis residue rich in lignin

Yanqin Huang [a], Zhiguo Wei [a,b], Xiuli Yin [a,*], Chuangzhi Wu [a]

[a] Key Laboratory of Renewable Energy and Gas Hydrate, CAS, Guangzhou 510640, China
[b] Graduate University of Chinese Academy of Sciences, Beijing 100049, China

ARTICLE INFO

Article history:
Received 15 August 2011
Received in revised form 11 October 2011
Accepted 12 October 2011
Available online 19 October 2011

Keywords:
Acid hydrolysis residue
Pyrolysis
TGA
XRD
Char reactivity

ABSTRACT

Pyrolytic characteristics of acid hydrolysis residue (AHR) of corncob and pinewood (CAHR, WAHR) were investigated using a thermo-gravimetric analyzer (TGA) and a self-designed pyrolysis apparatus. Gasification reactivity of CAHR char was then examined using TGA and X-ray diffractometer. Result of TGA showed that thermal degradation curves of AHR descended smoothly along with temperature increasing from 150 °C to 850 °C, while a “sharp mass loss stage” for original biomass feedstock (OBF) was observed. Char yield from AHR (42.64–30.35 wt.%) was found to be much greater than that from OBF (26.4–19.15 wt.%). In addition, gasification reactivity of CAHR char was lower than that of corncob char, and there was big difference in micro-crystallite structure. It was also found that CAHR char reactivity decreased with pyrolysis temperature, but increased with pyrolysis heating rate and gasification temperature at 850–950 °C. Furthermore, CAHR char reactivity performed better under steam atmosphere than under CO_2 atmosphere.

© 2011 Elsevier Ltd. All rights reserved.

1. Introduction

Along with increasing global warming and oil shortage, the use of biofuels to replace petroleum transportation fuels such as gasoline has attracted much attention (Timilsina and Shrestha, 2011). Of all the biofuels, bioethanol and biobutanol has the potential to be a valuable substitute for gasoline as the current transportation system can be used with little moderations (Matsumoto et al., 2009). Currently, biofuel can be produced from either lingocellulosic biomass or grains (so-called “first generation” ethanol). Producing biofuel from lingocellulosic biomass rather than sugar or starch offers many distinct advantages, such as more available feedstocks at lower cost and less competition with food (Damartzis and Zabaniotou, 2011; del Campo et al., 2006; Demirbas, 2011). However, it should be noted that the production of ethanol from biomass is more complicated than the 1st generation ethanol production: the hydrolysis of cellulose in the lingocellulosic biomass to produce reducing sugars is always necessary before the fermentation of sugars to ethanol (del Campo et al., 2006; Demirbas, 2011; Ravindranath et al., 2011). Therefore, the cost of lingocellulosic ethanol production is relatively high based on current technologies, and the major problems are the low yield and high cost of the hydrolysis process.

Hydrolysis residue (HR) is a by-product of the hydrolysis process. About 40–45 wt.% of feedstock is presently obtained as residue from a wood-to-ethanol hydrolysis process (Håkansson, 2007). It represents a kind of biomass resource that is concentrated already and rich in lignin. If the HR can be effectively utilized, the cost of lingocellulosic ethanol production could be lower. Gasification provides a beneficial and realistic way to convert the HR to gaseous fuels, from which electricity, liquid fuels and chemicals can be produced (Eriksson et al., 2004; Håkansson, 2007). Since the components and structure of the HR are different from that of common biomass (Zhang, 2010), it is significant to explore pyrolytic characteristics of the HR in order to provide theoretical reference for industrial application.

To better understand pyrolytic behavior of the HR, two sets of experiments were carried out in this work with thermo-gravimetric analyzer (TGA) and a self-designed pyrolysis apparatus. First of all, the mass loss of the HR was determined by the TGA. Then the yield of pyrolysis products (i.e. char, tar and gas) and the formation of gaseous product under different pyrolysis temperature were examined using the pyrolysis apparatus. Furthermore, the gasification reactivity of char obtained under different pyrolysis conditions (temperature, heating rate) was also investigated using TGA.

2. Experimental

2.1. Materials

Two kinds of acid hydrolysis residues (AHR) were tested in this experiments: the AHR of pinewood (PAHR) and corncob (CAHR). PAHR was derived from a continous acid hydrolysis process of pinewood-to-ethanaol. Thereinto, pinewood was selected from

---

* Corresponding author. Address: No. 2, Nengyuan Rd., Wushan Tianhe District, Guangzhou 510640, China. Tel.: +86 02087057731; fax: +86 02087057737.
E-mail address: xlyin@ms.giec.ac.cn (X. Yin).

0960-8524/$ - see front matter © 2011 Elsevier Ltd. All rights reserved.
doi:10.1016/j.biortech.2011.10.027

Shanghai province (China), and hydrolysis conditions used were 2% H_2SO_4, 10 min at 200 °C. CAHR was derived from a continuous acid hydrolysis process of corncob-to-butanol. Thereinto, corncob was selected from Liaoning province (China), and hydrolysis conditions used were 2% H_2SO_4, 20 min at 180 °C. The AHR (PAHR, CAHR), and their original materials (pinewood, corncob), were crushed, sieved and the size fraction of (150–250 μm) was chosen as samples. The proximate, ultimate and component analyzes of these samples are listed in Table 1. It is found that the AHR has higher lignin content (~50 wt.%) and higher ratio of C:H compared with original biomass.

2.2. TG analysis

Thermogravimetric analyzer (NETZSCH STA409C/PC) was used to investigate the mass loss stages of both AHR and their original material. In the TGA experiment, the samples were heated from 30 °C to 900 °C with a heating rate of 10 K min^{-1} under inert atmosphere with a N_2 flow rate of 60 ml min^{-1}. In each case, the mass of sample was less than 10 mg to avoid possible temperature gradient in the sample and to ensure kinetic control of the process.

2.3. The pyrolysis experiment

2.3.1. The apparatus and pyrolysis procedure

The pyrolysis apparatus, which has been described in detail previously (Huang et al., 2009a,b), was employed to investigate the pyrolysis behavior of AHR and its original biomass at temperatures ranging from 550 °C to 850 °C. Briefly, it was comprised of an electric heating furnace, a temperature control system, a 600 mm $(L) \times 35$ mm (I.D.) quartz tube reactor, and a sample container. In brief, about 1 g of the biomass sample was loaded into a quartz glass container and then placed at the cold side of the quartz tube. The gas temperature in the heated zone of the reactor was then increased and continuously monitored using K-type thermocouples. Once the reactor had stabilized at the desired temperature, the sample holder assembly was put into the heated zone and kept there for about 1–2 min to ensure complete conversion.

2.3.2. The yield of products

The yield of gaseous products was calculated based on the density and volume of the collected gas mixture. The density was found from the composition analysis of the mixture by GC (20B, Shimadzu) while the volume was measured by drainage. The yield of char residue was evaluated by the weight difference of sample container before and after the experiment while the tar yield was determined by mass balance.

Table 1
Proximate, ultimate and component analyzes of samples.

	PAHR	Pinewood	CAHR	Corncob
Proximate analysis (w_{ad}%)				
Moisture	9.97	12.36	8.19	4.43
Volatiles	58.73	64.66	61.64	75.84
Fixed carbon	29.61	20.27	28.92	17.37
Ash	1.69	2.71	1.25	2.36
Ultimate analysis (w_{daf}%)				
C	55.00	49.13	53.66	46.43
H	5.29	6.76	5.34	5.78
O[a]	35.87	40.94	40.80	47.69
N	3.26	3.08	0.04	0.08
S	0.58	0.09	0.16	0.02
C/H	10.40	7.27	10.05	8.10
Low heating value (MJ/kg)	22.73	18.21	20.94	17.39
Component analysis (w_{ad}%)				
Hemicellulose	7.84	19.56	8.83	39.85
Cellulose	28.67	36.40	28.18	36.47
Lignin	51.83	28.97	47.84	13.52

ad, air dry basis; daf, dry and ash-free basis.
[a] By difference.

2.4. Char reactivity

2.4.1. Char preparation

Char was prepared at different temperatures (650 °C, 750 °C, 850 °C) and heating rates (0.1 K/s, 15 K/s) using the self-designed pyrolysis apparatus (Section 2.3.1). Typically, about 12 g of the biomass sample was loaded into a quartz glass container and then placed in the center of the quartz tube. The sample was then heated at a heating rate of 0.1 K/s to a final temperature of 650 °C, 750 °C, or 850 °C, and held at each temperature for 50 min under a continuous flow of nitrogen of 400 ml min^{-1}. The pyrolysis temperature and heating rate were controlled with a power control system and the operation temperature was continuously monitored by a K-type thermocouple inserted into the sample container.

When char was prepared at ~15 K/s, about 1 g of the biomass sample was loaded into a quartz glass container and then placed at the cold side of the quartz tube. The gas temperature in the heated zone of the reactor was then increased and continuously monitored using K-type thermocouples. Once the reactor had stabilized at the desired temperature, the sample holder was put into the heated zone and kept there for about 1–2 min to ensure complete conversion.

At the end of each run, the product char was cooled to ambient temperature. Char yield was calculated from the amount of char based on the initial mass of the unpyrolyzed CAHR. The yield of char was used as an index for the reproducibility of experiments. Chars pyrolyzed under the same conditions were considered to be identical only if the difference in yield was less than 2%.

2.4.2. XRD analysis

The crystal structure, crystallite size and residual strain information were determined using X-ray diffractometer (Rigaku D/max-IIIA). XRD measurements were performed at a voltage of 40 kV and a current of 30 mA using a diffractometer containing a Cu target tube and a graphite monochromator. The XRD profiles were recorded from 5° to 80° at a scanning speed of 8°min^{-1}.

The characteristic size of chars, including distance between aromatic layers (d_{002}), layer diameter (L_a) and average thickness of conglomerate deposit (L_c) were calculated with Scherrer formula and Bragg equations

$$d_{002} = \frac{\lambda}{2\sin\theta_{002}} \tag{1}$$

$$L_a = \frac{K_2\lambda}{\beta_{100}\cos\theta_{100}} \tag{2}$$

$$L_c = \frac{K_1\lambda}{\beta_{002}\cos\theta_{002}} \tag{3}$$

where λ is wave-length of incident wave (A, $\lambda = 1.54178$), 2θ is diffraction angle (°), β is half-width of diffraction peak (rad), K_1 and K_2 are constants of wave form factors.

2.4.3. Char reactivity measurement using TGA

Char reactivity was measured in CO_2 and steam atmosphere at 850 °C, 900 °C, and 950 °C using a thermo-gravimetric analyzer (STA449 F3, NETZSCH). Briefly, char sample was loaded in an alumina pan and heated under N_2 flow of 60 ml/min to the designated temperature of 850 °C, 900 °C and 950 °C at a rate of 40 °C/min. Then the atmosphere for the sample was switched to CO_2 or steam from N_2, and the sample was allowed to gasify until its weight remained unchanged. In all cases, the flow rate of CO_2 was usually

150 ml/min and the mass of the sample was less than 10 mg to ensure the kinetic control of the reaction process. The carbon conversion ratio (x_t, 100%) and gasification rate (r_t, min^{-1}) were then calculated using the following equations:

$$x_t = \frac{w_0 - w_t}{w_0 - w_{ash}} \tag{4}$$

$$r_t = -\frac{1}{w_0 - w_{ash}} \cdot \frac{dw_t}{dt} = \frac{dx_t}{dt} \tag{5}$$

where w_0 denotes the sample mass (mg) at the start of the gasification, w_t is sample mass at gasification time t, w_{ash} is the mass of ash remained after complete gasification.

3. Results and discussion

3.1. The pyrolysis characteristic using TGA

The TG and DTG curves for samples under nitrogen at 10 °C min^{-1} are shown in Fig. 1a and b. A “sharp mass loss stage” for the original biomass (i.e. corncob and pinewood) is observed within a narrow temperature zone of 260–420 °C, where the sample was decomposed and the volatile matters were released. On the other hand, the mass loss curves (TG curves) of AHR are found to decay smoothly from 150 °C to the final temperature 850 °C. It should be noted that char residue is one of the main products from AHR pyrolysis, accounting for about 30 wt.% of the feedstock, while the char residue yield from original biomass pyrolysis is about 20 wt.%. The high char residue yield of AHR is mainly ascribed to the high lignin content (Table 1), which tends to be carbonized through cross-link reaction compared to hemicelluloses and cellulose (Shen et al., 2009, 2010a). A notable mass loss peak, appearing at 320 °C for corncob and 358 °C for pinewood, is found at the major pyrolysis stage. The mass loss peak, corresponding to the cracking of the main lignin chain, is also found for AHR and appears at 398 °C for CAHR and 358 °C for PAHR, respectively. It should be noted that the mass loss peaks of untreated biomass (pinewood, corncob) is much notable than that of AHR. The reason for this is that untreated biomass has a high content of cellulose and hemicellulose, which are of sharper mass loss peaks than lignin (Huang et al., 2011a,b). Further examination shows that another visible peak appears at 202 °C on the DTG curve of CAHR. This is mainly ascribed to the decomposition of the side units (acetyl groups) (Shen et al., 2010b).

3.2. The fast pyrolysis experiment

3.2.1. Product distribution

The two kinds of AHR materials, CAHR and WAHR, were tested in the fast pyrolysis unit to investigate the effect of temperature on product yield. Fig. 2 shows the yield of char, gas, and tar from pyrolysis of CAHR and PAHR under the temperature from 550 °C to 850 °C. It is found that more AHR are converted to gas at high temperature and char yield decreases (especially over 650 °C), which was consistent with biomass as literature report (Bu et al., 2011). The yield of tar from CAHR reaches maximum (36.88 wt.%) at ~650 °C followed by a gradual decline, while that from PAHR changes slightly before 650 °C followed by a visible decrease, and then decreases gradually at the temperature over 750 °C. Consequently, it is also found that the gas yield from PAHR at higher temperature increases in proportion to the decreased tar production, which clearly demonstrates the competitive formation of tar over the condensable products reported by Sepman and de Goey (2011).

The pyrolysis characteristic of the original biomass feedstock (i.e. corncob) was also investigated to compare with that of AHR. Table 2 shows the product yield from pyrolysis of CAHR and corncob at different temperature. Generally, the gas yield from CAHR is less than that from corncob at 550–850 °C, while the char yield from the two kinds of materials behaves differently. Furthermore, it is found that before 750 °C the tar yield from CAHR is less than that from corncob, and then there is a noticeably decrease in corncob char yield at 750 °C. The great difference in product distribution between CAHR and corncob may be ascribed to different component contents (shown in Table 1). It was reported that lignin performed a high yield of char (about 36% for kraft lignin at 825 °C) (Shen et al., 2010b), while hemi-cellulose and cellulose were inclined to produce liquids and gaseous products (Shen et al., 2010a). Another reason for the distribution difference mentioned above may be that structure of AHR were destroyed and reformed during hydrolysis process, which needs to be further explored.

Furthermore, it needs to be noted that the formation of char from CAHR (42.64–30.35%) is much greater than that from corncob (26.40–19.15%), owning to high lignin content in CAHR (47.84% for CAHR, 13.52% for corncob), similar to results from Zhang et al. (2008).

3.2.2. The gaseous products

The volume yields of the main products (H_2, CO, CH_4 and CO_2) from CAHR along with pyrolysis temperature of 550–850 °C are shown in Fig. 3. It is apparent that the yields of CO and CO_2 are

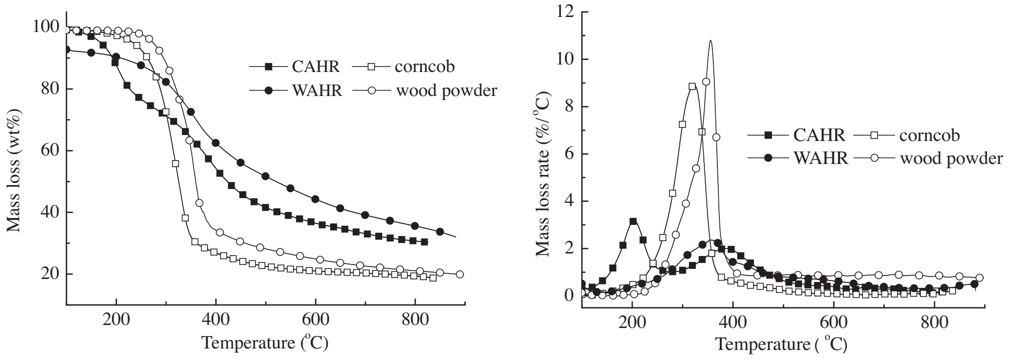

(a) **(b)**

Fig. 1. TG and DTG curves of corncob, CAHR, pinewood and PAHR: (a) TG and (b) DTG.

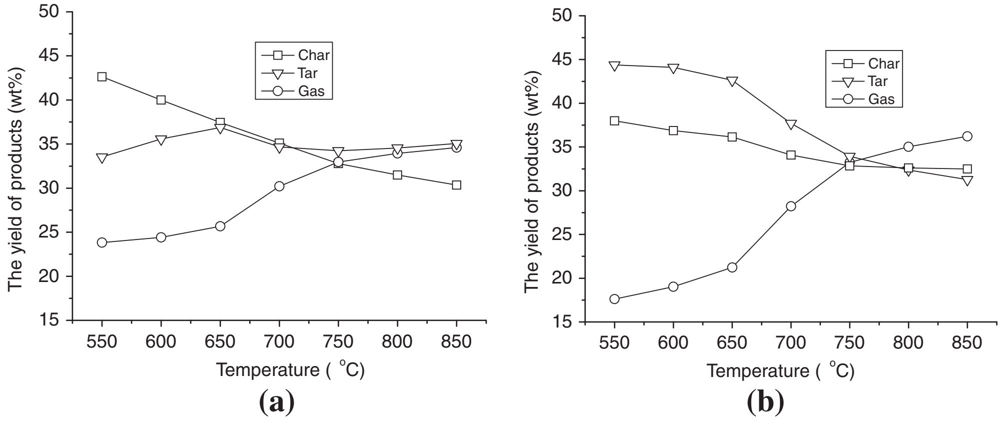

Fig. 2. The yield of char, gas and tar from pyrolysis of AHR at different temperature: (a) CAHR and (b) PAHR.

Table 2
The product from pyrolysis of CAHR and corncob at different temperature.

Product (wt.%)	Pyrolysis temperature (°C)							
	550		650		750		850	
	CAHR	Corncob	CAHR	Corncob	CAHR	Corncob	CAHR	Corncob
Gas	23.83	31.99	25.68	37.82	32.97	50.79	34.59	51.16
Tar	33.53	41.60	36.88	40.48	34.24	29.66	35.06	29.05
Char	42.62	26.40	37.44	21.69	32.79	20.16	30.35	19.18

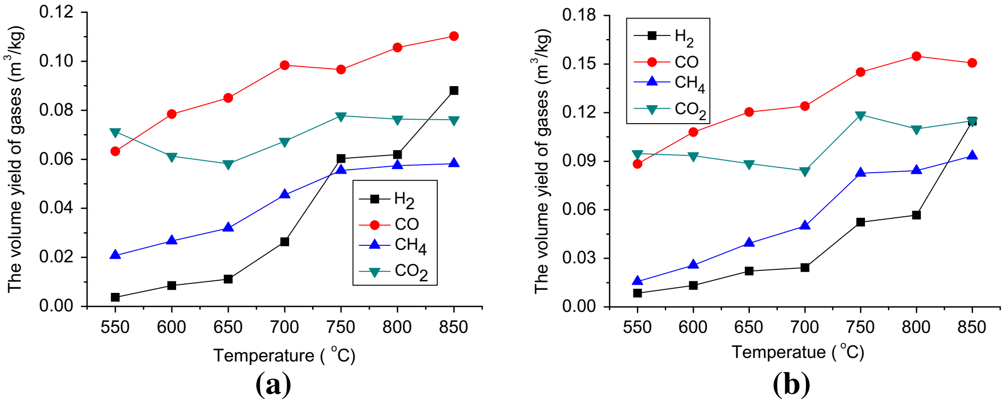

Fig. 3. The volume yield of gases from CAHR and corncob under different temperature: (a) CAHR and (b) corncob.

much higher than H_2 and CH_4 before 650 °C. When at elevated temperature over 650 °C the formation of H_2 significantly increases (0.011 m^3/kg at 650 °C compared with 0.062 m^3/kg at 750 °C), due to the cleavage of the C=C and C–H bonds linked to phenyl ring from lignin. It needs to be noted that another noticeably increase of H_2 production is observed at over 800 °C, which is mainly ascribed to reaction of char with H_2O. The yield of CO is enhanced at the elevated temperature and reaches 0.099 m^3/kg at 700 °C due to cleavage of carbonyl group from cellulous. At over 700 °C the production of CO decreases slightly and then is enhanced, which is ascribed to competition between water–gas shifting reaction and the reaction of char with H_2O. Comparatively, the yield of CO_2 behaves differently from that of CO. Furthermore, the production of CH_4 is enhanced from 0.021 m^3/kg to 0.058 m^3/kg along with temperature increasing from 550 °C to 850 °C.

Fig. 3b shows the evolution of H_2, CO, CH_4 and CO_2 from corncob at different temperature. By comparing Fig. 3b with Fig. 3a, it is obvious that the variation of gas yield along with increasing temperature from corncob performs in accord with that from CAHR. Furthermore, it should be noted that under pyrolysis temperature the yield of CO from corncob is greater than that from CAHR, so are the yield of H_2, CH_4, and CO_2. This is mainly ascribed to high content of hemicellulose which favored formation of low molecular weight products (Haykiri-Acma et al., 2010).

3.3. Char characteristics

Char yield from AHR pyrolysis, accounting for about 30–50 wt.% of the AHR, was much higher than that from common biomass pyrolysis. It is known that devolatilization is a prior step of biomass gasification and the char is an intermediate solid residue. Therefore, conversion level of the char in the gasification step determines the overall efficiency of the gasifier. Furthermore, the char conversion depends on its reactivity which is a function of pyrolysis conditions (Baratieri et al., 2008; Lv et al., 2010), such as the heating rate, pyrolysis temperature. Therefore, the reactivity

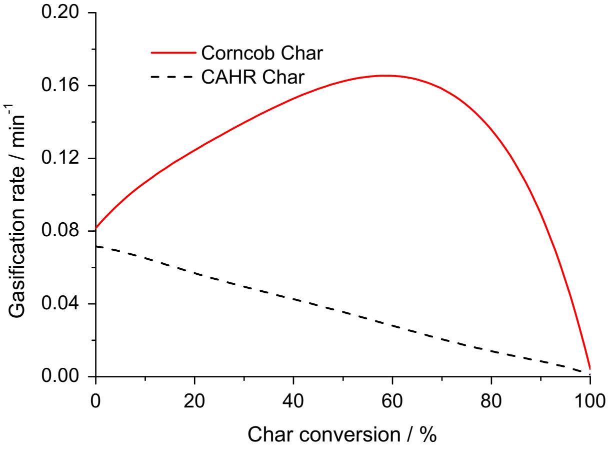

Fig. 4. The CO_2 gasification reactivity of CAHR and corncob chars as a function of char conversion.

of CAHR char was investigated in the study in order to better understand AHR char reactivity.

3.3.1. The reactivity of char from CAHR and corncob

The gasification reactivity of chars, from CAHR and corncob pyrolyzed at 650 °C, was evaluated using a TGA in CO_2 atmosphere at 900 °C. Fig. 4 depicts CO_2 gasification reactivity of chars from CAHR and corncob char as a function of char conversion. It shows that during the whole reaction process, CO_2 gasification rate of CAHR char is much lower than that of corncob char at the same char conversion. Furthermore, it is notable that the gasification rate of CAHR char decrease along with char conversion, while that of corncob char increases and reaches a maximum at char conversion of 58% followed by a gradually decrease. Generally, it can be concluded that CAHR char is being of lower gasification reactivity than corncob char, therefore, in order to achieve high carbon conversion rate, longer residence time for CAHR char in gasifier is needed during its gasification process.

The char reactivity is greatly influenced by its structural feature as reported by Lv et al. (2010). Therefore, in order to further understand the big difference existing in char reactivity between CAHR and corncob, the XRD spectra of chars derived from CAHR and corncob, were investigated. The characteristic micro-crystallite parameters, calculated by Scherrer formula and Bragg equations, are summarized in Table 3.

It was found that CAHR char had higher 002-peak (at $2\theta = 23.5°$) and 100-peak (at $2\theta = 43.5°$) than corncob char, which indicated that the CAHR char had a greater degree of order in the carbon structure. In addition to the peaks C(002) and C(100), more spiculate peaks were observed in the XRD spectrum of corncob char. The spiculate peaks were crystal structure formed by alkali (K) and alkaline-earth (Ca) metals existing in corncob. It was reported that the crystal structure of these metals provided active site for reaction of char with gas, thus enhanced its gasification reactivity (Huang et al., 2009a,b).

Table 3 shows important parameters (L_a, L_c and d_{002}) for describing crystallite structure of graphite formed in the chars (Pang et al., 2007). It can be seen that the aromatic layer diameters (L_a) of CAHR char is much higher than that of corncob char, indicating that CAHR char is of a higher condensation degree. It should be noted that CAHR char has a higher average accumulating layer (L_c/d_{002}) than corncob char. It was reported higher (L_c/d_{002}) meant higher crystallite structure (Pang et al., 2007). It can be concluded that, during CAHR pyrolysis, higher crystallite structure was formed due to its high lignin content, and this reduced contact chance of char and gas. Therefore, the reactivity of CAHR char is lower than that of corncob char. In addition, the values of average accumulating layer (L_c/d_{002}) in both chars are less than 2, which is much lower than that of coal chars (about 6) and consistent with reported results (Zhang et al., 2010; Min et al., 2008).

Table 3
The micro-crystallite parameters of char samples.

Char samples	d_{002} (nm)	L_c (nm)	L_a (nm)	L_c/d_{002}
CAHR	0.385	0.756	3.812	1.97
Corncob	0.377	0.630	2.914	1.67

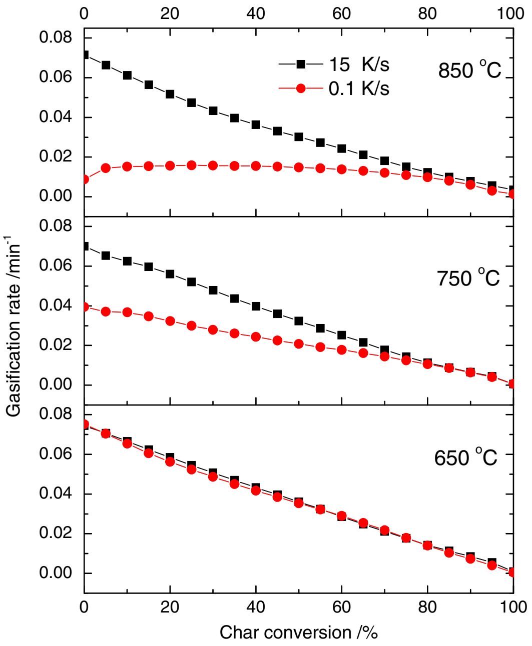

Fig. 5. The CO_2 gasification reactivity of CAHR char at different gasification temperature at different pyrolysis conditions.

3.3.2. The effect of pyrolysis conditions

Fig. 5 shows comparison of CO_2 reactivity of char prepared at different temperatures (650 °C, 750 °C, 850 °C) and heating rates (0.1 K/s, 15 K/s). It can be seen that char reactivity decreases along with pyrolysis temperature from 650 °C to 850 °C, and the reactivity of char from15 K/s is higher than that from 0.1 K/s. When CAHR was heated at a high heating rate, the volatiles were released rapidly, and char agglomeration and condensation of fragments on the char surface were prevented (Fushimi et al., 2003). Thus, char surface with some macropores was formed (Huang et al., 2009a,b). But during slow pyrolysis, volatiles evolution was very slow and this increased chance of repolymerization of volatiles to the char (Lv et al., 1996; Yang et al., 2007). Furthermore, because of long heating time during slow pyrolysis, crystallite structure of graphite was formed in char and its degree was higher than that generated at rapid heating rate (Cetin et al., 2004; Huang et al., 2009a,b). Therefore, the char from15 K/s is of higher reactivity than that from 0.1 K/s. Fushimi et al. (2003) also found that the reactivity of char rapidly heated was higher when they studied lignin and bagasse.

In addition, it should be noted that the reactivity difference between in chars pyrolyzed at 15 K/s and 0.1 K/s is increasing as pyrolysis temperature increases from 650 °C to 850 °C. Moreover, the effect of pyrolysis temperature on char reactivity at 0.1 K/s is

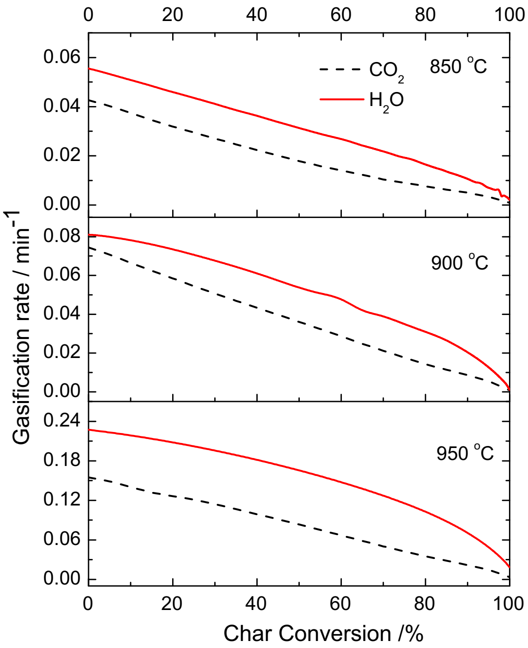

Fig. 6. The reactivity of CAHR char as a function of char conversion at different gasification conditions.

greater than that at 15 K/s. During slow pyrolysis, when temperature increased from 650 °C to 850 °C, the heating time of char increased obviously because of lower heating rate (0.1 K/s). Then the crystallite structure of graphite in the char was strengthened, which has a negative impact on char reactivity (Cetin et al., 2004).

3.3.3. The effect of gasification conditions

Fig. 6 shows reactivity of CAHR char at different gasification temperatures of (850 °C, 900 °C, 950 °C) under CO$_2$ and steam atmosphere. It is found that both the CO$_2$ and steam reactivity of CAHR char increase with gasification temperature from 850 °C to 950 °C, indicating reactions under kinetic control. In addition, it is notable that char has a higher gasification rate under steam atmosphere than that under CO$_2$ atmosphere. This can be explained that: (1) steam has a smaller molecular diameter than CO$_2$, which enhances contact chance of char and steam, and (2) during steam gasification, more new pores were formed and this provided more reaction active sites for char and steam (Huang et al., 2011a,b). So the rate of gasification with steam is higher than that with CO$_2$. Furthermore, it should be noted that the CO$_2$ gasification rate of char decreases linearly with increasing char conversion, while gasification rate of char under steam atmosphere decrease slower along with char conversion especially at high temperature. It shows that steam gasification rate of char is higher during whole reaction process at 950 °C. To sum up, it can be concluded that steam gasification at high temperature can accelerate CAHR gasification.

4. Conclusion

Extensive experiment study was carried out to investigate pyrolysis characteristics of CAHR and PAHR. Thermal degradation curves of AHR decayed smoothly with temperature increasing from 150 °C to 850 °C due to its high lignin content. Yield of gaseous product from AHR pyrolysis was lower than that from OBF, while the formation of char from AHR was much higher than that from OBF. Gasification reactivity of CAHR char was relatively low and it can be effectively improved through steam gasification at high temperature. Therefore, for AHR gasification, steam gasification at high temperature is a good choice, and long residual time in gasifier is also preferred.

Acknowledgements

The authors gratefully acknowledge the financial support from the National Natural Sciences Foundation of China (50876109) and the National Key Technology Research and Development Program of China (2011BAD22B06).

References

Baratieri, M., Baggio, P., Fiori, L., Grigiante, M., 2008. Biomass as an energy source. Thermodynamic constraints on the performance of the conversion process. Bioresour. Technol. 99 (15), 7063–7073.

Bu, Q., Lei, H.W., Ren, S.J., Wang, L., Holladay, J., Zhang, Q., Tang, J.M., Ruan, R., 2011. Phenol and phenolics from lignocellulosic biomass by catalytic microwave pyrolysis. Bioresour. Technol. 102 (13), 7004–7007.

Cetin, E., Moghtaderi, B., Gupta, R., Wall, T.F., 2004. Influence of pyrolysis conditions on the structure and gasification reactivity of biomass chars. Fuel 83 (16), 2139–2150.

Damartzis, T., Zabaniotou, A., 2011. Thermochemical conversion of biomass to second generation biofuels through integrated process design – a review. Renew. Sust. Energy Rev. 15 (1), 366–378.

del Campo, I., Alegría, I., Zazpe, M., Echeverría, M., Echeverría, I., 2006. Diluted acid hydrolysis pretreatment of agri-food wastes for bioethanol production. Ind. Crop Prod. 24 (3), 214–221.

Demirbas, A., 2011. Competitive liquid biofuels from biomass. Appl. Energy 88 (1), 17–28.

Eriksson, G., Kjellström, B., Lundqvist, B., Paulrud, S., 2004. Combustion of wood hydrolysis residue in a 150 kW powder burner. Fuel 83 (11–12), 1635–1641.

Fushimi, C., Araki, K., Yamaguchi, Y., Tsutsumi, A., 2003. Effect of heating rate on steam gasification of biomass. 1. Reactivity of char. Ind. Eng. Chem. Res. 42 (17), 3922–3928.

Håkansson, K., 2007. Torrefaction and gasification of hydrolysis residue. Vol. Master, Umeå Institute of Technology.

Haykiri-Acma, H., Yaman, S., Kucukbayrak, S., 2010. Comparison of the thermal reactivities of isolated lignin and holocellulose during pyrolysis. Fuel Process. Technol. 91 (7), 759–764.

Huang, Y., Yin, X., Wu, C., Wang, C., Xie, J., Zhou, Z., Ma, L., Li, H., 2009a. Effects of metal catalysts on CO$_2$ gasification reactivity of biomass char. Biotechnol. Adv. 27 (5), 568–572.

Huang, Y., Yin, X., Wu, C., Wang, C., Xie, J., Zhou, Z., Ma, L., Li, H., 2009b. Study on CO$_2$ gasification reactivity of rice straw chars. J. Fuel Chem. Technol. 37 (3), 289–295.

Huang, Y.F., Kuan, W.H., Chiueh, P.T., Lo, S.L., 2011a. A sequential method to analyze the kinetics of biomass pyrolysis. Bioresour. Technol. 102 (19), 9241–9246.

Huang, Y., Su, D., Yin, X., Wu, C., Ma, L., 2011b. Changes of pore structure and gasification reactivity during CO$_2$ and H$_2$O gasification of fir char [J]. J. Fuel Chem. Technol. 39 (6), 432–437.

Lv, X.Z., Huang, Y.H., Yan, Y.J., Cai, G.C., 1996. Technological properties of flash pyrolyzed chars. J. East China Univ. Sci. Technol. 22, 136–141.

Lv, D., Xu, M., Liu, X., Zhan, Z., Li, Z., Yao, H., 2010. Effect of cellulose, lignin, alkali and alkaline earth metallic species on biomass pyrolysis and gasification. Fuel Process. Technol. 91 (8), 903–909.

Matsumoto, N., Sano, D., Elder, M., 2009. Biofuel initiatives in Japan: strategies, policies, and future potential. Appl. Energy 86 (Suppl. 1), S69–S76.

Min, F., Zhang, M., Chen, Q., 2008. Study on pyrolysis gasification semicoke characteristics of fresh biomass by FTIR. J. Anhui Univ. Sci. Technol. 2, 55–58.

Pang, K.L., Zhao, C.S., Lin, L., 2007. XRD and gasification characteristic of natural coke. J. Fuel Chem. Technol. 35 (3), 268–272.

Ravindranath, N.H., Sita Lakshmi, C., Manuvie, R., Balachandra, P., 2011. Biofuel production and implications for land use, food production and environment in India. Energy Policy. 39 (10), 5737–5745.

Sepman, A.V., de Goey, L.P.H., 2011. Plate reactor as an analysis tool for rapid pyrolysis of biomass. Biomass Bioenergy 35 (7), 2903–2909.

Shen, D.K., Gu, S., Luo, K.H., Bridgwater, A.V., Fang, M.X., 2009. Kinetic study on thermal decomposition of woods in oxidative environment. Fuel 88 (6), 1024–1030.

Shen, D.K., Gu, S., Bridgwater, A.V., 2010a. The thermal performance of the polysaccharides extracted from hardwood: cellulose and hemicellulose. Carbohydr. Polym. 82 (1), 39–45.

Shen, D.K., Gu, S., Luo, K.H., Wang, S.R., Fang, M.X., 2010b. The pyrolytic degradation of wood-derived lignin from pulping process. Bioresour. Technol. 101 (15), 6136–6146.

Timilsina, G.R., Shrestha, A., 2011. How much hope should we have for biofuels? Energy 36 (4), 2055–2069.

Yang, F., Zhou, Z.J., Wang, F.C., Liu, H.F., Gong, X., Yu, Z.H., 2007. Characteristic of the Shenfu coal chargasification with steam and carbon dioxide. J. Fuel Chem. Technol. 35, 660–666.

Zhang, B., 2010. Study on physicochemical properties and pyrolysis characteristics of wood powder acid hydrolysis residue and its isolated acidolysis lignin. Vol. Doctor, Guangzhou Institute of Energy Conversion, Chinese Academy of Sciences, Guangzhou.

Zhang, H.X., Yang, Z.G., Zhang, B.G., Chen, X., Bai, Z.H., 2008. Studies on pyrolysis of wheat straw residues from ethanol production by solid-state fermentation. J. Anal. Appl. Pyrol. 81 (2), 243–246.

Zhang, B., Yin, X., Wu, C., Qiu, Z., Xie, J., Wang, C., Ma, L., Wu, S., 2010. Research on pyrolysis characteristics of hydrolysis residues of wood powder. Acta Energiae Solaris Sinica 31 (10), 1125–1229.